Positron and electron backscattering from elemental solids in the 1–10 keV energy range

2004 J. Phys.: Condens. Matter 16 799

(http://iopscience.iop.org/0953-8984/16/6/010)

INSTITUTE OF PHYSICS PUBLISHING JOURNAL OF PHYSICS: CONDENSED MATTER

J. Phys.: Condens. Matter **16** (2004) 799–808 PII: S0953-8984(04)71887-1

Positron and electron backscattering from elemental solids in the 1–10 keV energy range

Z Chaoui[1] **and N Bouarissa**[2,3]

[1] Physics Department, Faculty of Science, University of Setif, 19000 Setif, Algeria
[2] Physics Department, Faculty of Science and Engineering, University of M'Sila, 28000 M'Sila, Algeria

E-mail: z_chaoui@yahoo.fr and n_bouarissa@yahoo.fr

Received 12 November 2003
Published 30 January 2004
Online at stacks.iop.org/JPhysCM/16/799 (DOI: 10.1088/0953-8984/16/6/010)

Abstract

Electron and positron backscattering coefficients are analytically calculated for a number of selected atomic targets in the energy range 1–10 keV and for incident angles between 0° and 80°. The dependence of the backscattering coefficient on the material, on the projectile primary energy and on the incidence angle has been examined and discussed. Our results are found to be in better agreement with experiment than earlier Monte Carlo simulations.

1. Introduction

The interaction of slow charged particles such as electrons and positrons with solid targets is of prime importance in many areas of surface science, solid state physics and microelectronics [1–11]. The problem, which is not new, has received recent attention because of its importance in electron spectroscopy, electron microlithography, positron annihilation spectroscopy and so on [8–15]. Indeed, backscattered electrons from solid targets are utilized to obtain the backscattered electron image in scanning electron microscopy and to detect registration marks in electron beam lithography [16], while positrons have been used in many ways as a probe of surfaces or thin films [17–19]. There may be a possibility of using the positron beams as industrial analysis tools [11]. Of more fundamental scientific importance, the combined study of electron and positron backscattering provides a rare opportunity to establish detailed interaction cross sections, since it is the simplest matter–antimatter system which can be routinely obtained and controlled in a modest laboratory [20]. In fact, an understanding of positron collision processes in solids underpins and strengthens the description of equivalent electron processes which govern the interpretation of an array of techniques using mono-energetic electrons as probes of solid samples [21].

[3] Author to whom any correspondence should be addressed.

The knowledge of the collision processes can be encapsulated in scattering cross sections that can be used to find either the electron or positron trajectories in a Monte Carlo simulation [13–16, 20–32] or to obtain stopping powers and transport cross sections needed for analytic transport theory [6, 33]. Backscattering coefficients for electrons and/or positrons impinging on solid targets may provide stringent tests on the accuracy of the description of the scattering processes. Calculations of electron and positron backscattering coefficients as a function of both incident angles and target atomic number Z for a large range of energies have been made by several authors [6, 14, 20, 21, 23, 27–29, 31, 32, 34, 35]. More general theoretical problems of calculating transmission, backscattering and absorption of electrons impinging on supported and unsupported thin films have been also reported [30, 36–38]. However, relatively few data exist for low energy electrons and positrons.

In the present work, we have investigated theoretically the backscattering of electrons and positrons incident normally and obliquely on metallic targets in the energy range up to 10 keV. The dependence of the electron and positron backscattering coefficient and their ratio on both incident angles and target atomic number Z has been calculated. The computation of the range was performed using more realistic transport cross sections and Gaussian quadrature of the polynomial best fits of the stopping power numerical results given by Ashley [39]. The value of the backscattering coefficient has been obtained using the Vicanek and Urbassek theory [40] instead of Monte Carlo simulation.

More details about the method of calculations used in the present paper are given in section 2. Results of our calculations of the electron and positron backscattering coefficient and their ratio as a function of incident angles and Z are reported and compared where possible with measured and previously calculated data in section 3. Section 4 contains a conclusion.

2. Method of calculation

2.1. Backscattering coefficient

In the well known Vicanek and Urbassek theory, the backscattering coefficient function of the angle of incidence θ is expressed by [40]

$$\eta(\theta) = \left(1 + a_1\frac{\mu_0}{\upsilon^{1/2}} + a_2\frac{\mu_0^2}{\upsilon} + a_3\frac{\mu_0^3}{\upsilon^{3/2}} + a_4\frac{\mu_0^4}{\upsilon^2}\right)^{-1/2} \tag{1}$$

with: $\mu_0 = \cos(\theta)$ and $a_1 \approx 3.39$, $a_2 \approx 8.59$, $a_3 \approx 4.16$, $a_4 \approx 135.9$.

In expression (1), υ is the mean number of wide angle collisions defined as

$$\upsilon = NR\sigma_{\mathrm{tr}} \tag{2}$$

where N is the number of atoms per unit of volume and R is the range of penetration defined as

$$R = \int_{E_0}^{0} \frac{\mathrm{d}E}{\mathrm{d}E/\mathrm{d}s}. \tag{3}$$

For the energy lost per unit of length $\mathrm{d}E/\mathrm{d}s$, the best fits of the stopping power numerical results given by Ashley [39] are used for both electrons and positrons. The integration of the range is performed from the primary energy $E_0 = 10$ keV–100 eV. The termination energy is taken to be 100 eV since below this energy the maximum penetration length of the charged particle is just few ångströms [14].

2.2. The transport cross section

A non-relativistic treatment is used to evaluate the transport cross section for both electrons and positrons. The transport cross section used is expressed as the following series:

$$\sigma_{\mathrm{tr}} = 4\pi \sum_{l=0}^{\infty} (l+1) \sin^2(\delta_l - \delta_{l+1}). \tag{4}$$

The phase shifts δ_l have been obtained by numerically solving the Schrödinger equation of an electron (positron) with an atom bound in a solid. The potential considered is the effective scattering potential obtained from a density functional method [41, 42]. The solid effect due to the structure of the solid is included by superimposing atomic charge densities in the lattice [23] so that the Coulomb term is a superimposed potential calculated from the superposition of free-atom potentials.

In the case of electrons, the exchange effect is taken into account by adding the exchange expression of Furness and MacCarthy [43] to the Coulomb term. This expression has been used in a relativistic treatment by Dapor [6] and the results show better agreement with experiment than earlier work. The phase shifts are evaluated by numerically solving the Dirac equation.

For positrons, we have introduced the correlation effect using the interpolation formula deduced by Boronski and Nieminen [44] that is mainly based on the results of Arponen and Pajanne [45].

3. Results

3.1. Electron and positron backscattering coefficients

3.1.1. Normal incidence. In figure 1 the calculated electron backscattering coefficient η_- is represented, for various semi-infinite metals. The incidence is normal and the primary energies examined range from 1 to 10 keV. The solid curves shown for comparison are the experimental electron coefficients reported in [30]. From figure 1, one can note that our results are in very good agreement with the available experimental data. These results suggest that the behaviour of η_- depends on the target atomic number Z and hence on the elastic scattering cross section that is larger for heavy atoms. As in elastic collisions heavy atoms have a larger probability of scattering into large angles than the light atoms, one may expect η_- to become larger as Z becomes higher. This is clearly seen in figure 1.

Table 1 gives our theoretical results for the positron backscattering coefficient η_+ (referred to as PW) for various values of Z and for positron primary energy in the range 1–10 keV. For comparison, experimental and Monte Carlo (MC) simulations results for η_+ reported in [21] are also presented. There is very good agreement between our results and the available experimental ones. Moreover, our results are closer to experiment than those of the Monte Carlo simulations reported in [21], suggesting therefore that the use of the Vicanek and Urbassek model [40] with accurate transport cross sections as well as the use of Ashley functions for the stopping power make the calculation of the backscattering coefficients both less time-consuming and better as regards agreement with experiment.

One should note that our results shown in table 1 suggest a non-monotonically increasing dependence of η_+ on target atomic number Z for positron incident energies smaller than 3 keV. The non-monotonic increase of η_+ with Z seen at low energies (<3 keV) is not found for positron incident energies above 3 keV where we note a monotonic increase of η_+ with Z. At low energies (<4 keV; see table 1), the results of Coleman *et al* [21] showed that $\eta_+(z)$ is not a monotonic function of Z. For energies larger than 10 keV, they found a smooth, monotonically increasing dependence of η_+ on atomic number Z.

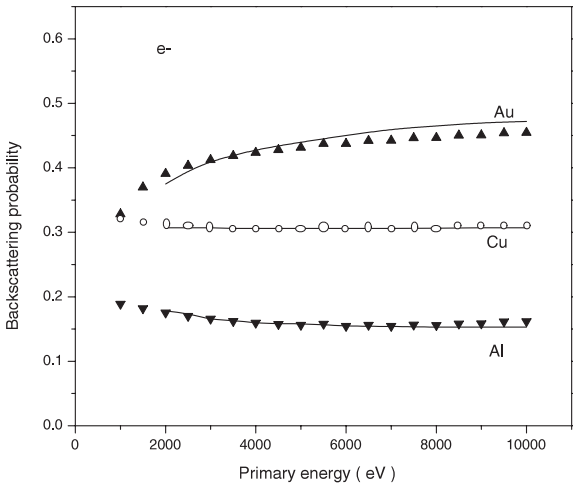

Figure 1. The electron backscattering coefficient, η_-, from targets of Al, Cu and Au. The solid curves are the experimental results reported in [29].

Table 1. Calculated (PW), experimental (Exp) [21] and simulation (MC) [21] results for positron backscattering coefficients in the energy range 1–10 keV for a variety of target species.

Z	E (keV)	1	2	3	4	5	6	7	8	9	10
13	PW	0.0864	0.0987	0.104	0.107	0.111	0.113	0.116	0.118	0.120	0.123
	Exp	0.069	—	0.086	—	0.112	—	0.122	—	—	0.123
	MC	0.109	—	0.115	—	0.126	—	0.125	—	—	0.128
29	PW	0.117	0.146	0.163	0.175	0.185	0.193	0.200	0.205	0.210	0.215
	Exp	0.135	—	0.177	—	0.205	—	0.226	—	—	0.229
	MC	0.156	—	0.194	—	0.205	—	0.231	—	—	0.235
47	PW	0.109	0.146	0.173	0.194	0.212	0.228	0.242	0.254	0.266	0.277
	Exp	0.106	—	0.168	—	0.227	—	0.243	—	—	0.277
	MC	0.126	—	0.182	—	0.216	—	0.236	—	—	0.245
79	PW	0.112	0.153	0.182	0.205	0.223	0.239	0.252	0.264	0.275	0.285
	Exp	0.123	—	0.186	—	0.232	—	0.273	—	—	0.294
	MC	0.168	—	0.242	—	0.290	—	0.316	—	—	0.340

3.1.2. Oblique angles of incidence. Figures 2(a) and (b) illustrate the dependence of calculated electron and positron backscattering coefficients on angle of incidence θ ($0^\circ \leqslant \theta \leqslant 80^\circ$ relative to the surface normal for the material of interest) for Al, Cu, Ag and Au for various energies in the range 1–10 keV. As θ increases, the backscattering coefficient for both electrons and positrons increases as well for all materials of interest (independently of Z). The electron and positron seem to behave in qualitatively the same way. For almost all materials of interest, the backscattering coefficients $\eta_-(\theta)$ and $\eta_+(\theta)$ vary slowly between 0° and 30°, but increase rapidly at larger angles. According to our calculations, the backscattering coefficient, for both electrons and positrons, when the angle of incidence is 80° is much larger than for normal incidence. Hence, the results are sensitive to the choice of the angle of beam incidence on the surface.

Table 2 gives the dependence of the backscattering coefficient of the 5 keV positrons impinging on Al (light element) and Au (heavy element) on the angle of incidence θ ($0^\circ \leqslant$

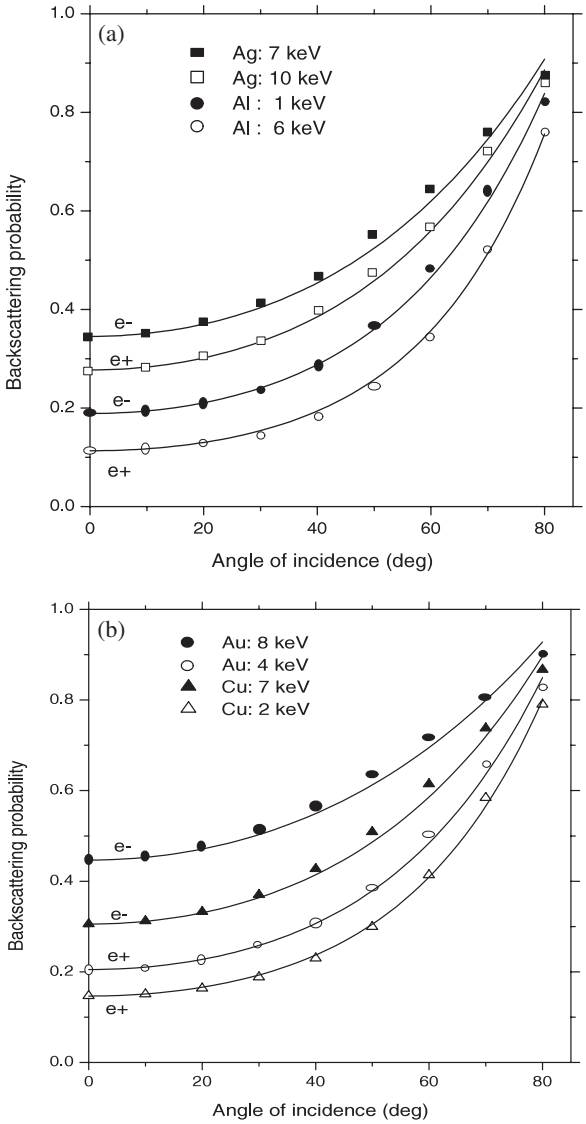

Figure 2. (a) Electron and positron backscattering coefficients, η_- and η_+ respectively, for targets of Al and Ag versus angle of incidence. The solid curves are the fits of the calculated backscattering coefficients to equation (5). (b) Electron and positron backscattering coefficients, η_- and η_+ respectively, for targets of Cu and Au versus angle of incidence. The solid curves are the fits of the calculated backscattering coefficients to equation (5).

$\theta \leqslant 80°$). Also shown for comparison are the measured and simulated positron coefficients $\eta_+(\theta)$ reported in [21]. Accordingly, the agreement between our calculated results and the available experimental ones is very good. It is noticeable that η_+ when the angle of incidence is 80° is about seven times η_+ for normal incidence in the case of Al, while it is about four times it in the case of Au. This could be due to the positrons having encountered several small angle scatterings and having lost more energy during the longer traversed path in the material, and also having a small total elastic scattering cross section, with the result that at non-normal incidence it is easier for positrons to scatter through more than 90° and to return

Table 2. Calculated (PW), experimental (Exp) [21] and simulation (MC) [21] results for positron backscattering coefficients versus angle of incidence for Al and Au at 5 keV.

		θ (deg)										
		0	10	20	30	40	50	55	60	65	70	80
Al	PW	0.111	0.114	0.124	0.143	0.177	0.237	0.281	0.341	0.419	0.517	0.754
	Exp	0.112	0.113	0.110	0.116	0.141	0.166	—	0.240	—	—	—
5 keV	MC	0.126	0.134	0.143	0.167	0.203	0.254	—	0.334	—	0.443	0.568
Au	PW	0.223	0.230	0.246	0.278	0.331	0.412	0.465	0.528	0.599	0.676	0.836
	Exp	0.232	0.256	0.247	0.256	0.326	0.426	0.468	—	0.553	—	—
5 keV	MC	0.290	0.295	0.301	0.336	0.369	0.422	—	0.478	—	0.552	0.673

into the vacuum than at normal incidence, which of course leads to the enhancement of the positron backscattering coefficient at non-normal incidence. One may then conclude that it is interesting to do experiments with a slow positron beam at normal incidence. Thus it is beneficial to use kiloelectronvolt positrons as a probe for obtaining information on the surface or near-surface region.

Following observations with electron beams [34, 47, 48] $\eta(\theta)$ varied with the angle to the surface normal, θ, according to the expression

$$\eta(\theta) = B\left(\frac{\eta_\perp}{B}\right)^{\cos\theta} \tag{5}$$

where B is a constant and $\eta_\perp$ is the backscattering coefficient at normal incidence.

The equation (5) has been fitted to our calculated electron backscattering coefficient $\eta_-(\theta)$. The results obtained regarding the fitted parameter B as a function of the electron primary energy for Al, Cu, Ag and Au are shown in figure 3(a). One can note that the parameter B is almost independent of the electron primary energy especially at energies greater than 2 keV but it depends on the target atomic number Z. From Monte Carlo calculations, Valkealahti and Nieminen [46] deduced that the expression (5) is correct for positrons as well. This relationship has also been used by Bouarissa *et al* [31] to fit their calculated Monte Carlo data as regards the positron backscattering probability $\eta_+(\theta)$. In the present work, fits of equation (5) to our calculated positron backscattering coefficient $\eta_+(\theta)$ have also been done. Our results concerning the dependence of the B parameter on the positron primary energy for the materials of interest are shown in figure 3(b). In figure 3(b), it is noticeable that generally the value of B increases very slightly with increasing positron incident energy, especially at low incident energies. This behaviour is qualitatively similar to that reported in [46] but, from the quantitative point of view, our values obtained for B are somewhat higher. This is due to our analytic backscattering coefficients being different from the Monte Carlo backscattering probabilities reported in [46]. However, we believe that our values for B are better than those reported in [46] since our backscattering coefficients are closer to the experimental ones.

3.2. Ratios of electron to positron backscattering coefficients

In figure 4(a) we display the variation of the ratio of the electron to positron backscattering coefficients (η_-/η_+) as a function of the projectile incident energy for Al, Cu, and Au at the normal angle of incidence. It is noticeable that the η_-/η_+ ratio rises significantly at low incident energies and has a constant value (which depends on the target atomic number Z) at high incident energies for all materials of interest. Coleman *et al* [21] show that this ratio rises significantly at low incident energies—e.g. closer to 2 at 5 keV.

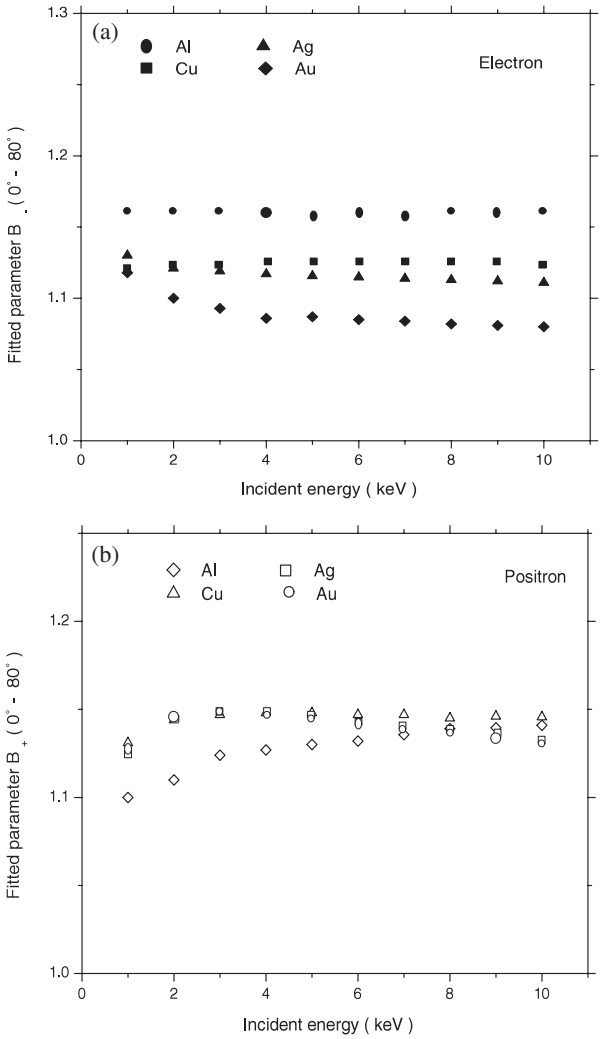

Figure 3. (a) Fitted parameter B_- deduced from equation (5) versus electron incident energy. (b) Fitted parameter B_+ deduced from equation (5) versus positron incident energy.

Figure 4(b) shows how the ratio of the electron to positron backscattering coefficients (η_-/η_+) varies with the angle of incidence θ for Cu, Ag and Au at the projectile incident energy of 6 keV. As the angle of incidence increases going from 0° to 80°, η_-/η_+ decreases for all materials under study.

According to expression (5), $\eta_-(\theta)/\eta_+(\theta)$ could be written as

$$\frac{\eta_-(\theta)}{\eta_+(\theta)} = B_\mp \left(\frac{\eta_\mp^\perp}{B_\mp} \right)^{\cos\theta} \tag{6}$$

where $B_\mp = \frac{B_-}{B_+}$ and $\eta_\mp^\perp = \frac{\eta_-^\perp}{\eta_+^\perp}$.

This relationship has been fitted to our calculated ratios of electron to positron backscattering coefficients. The results obtained for $B_\mp = B_-/B_+$ as a function of the projectile primary energy for Cu, Ag and Au are shown in figure 5. It appears that $B_\mp$ is almost constant at incident energies larger than 2 keV. On going from 2 to 4 keV, it decreases slightly. The

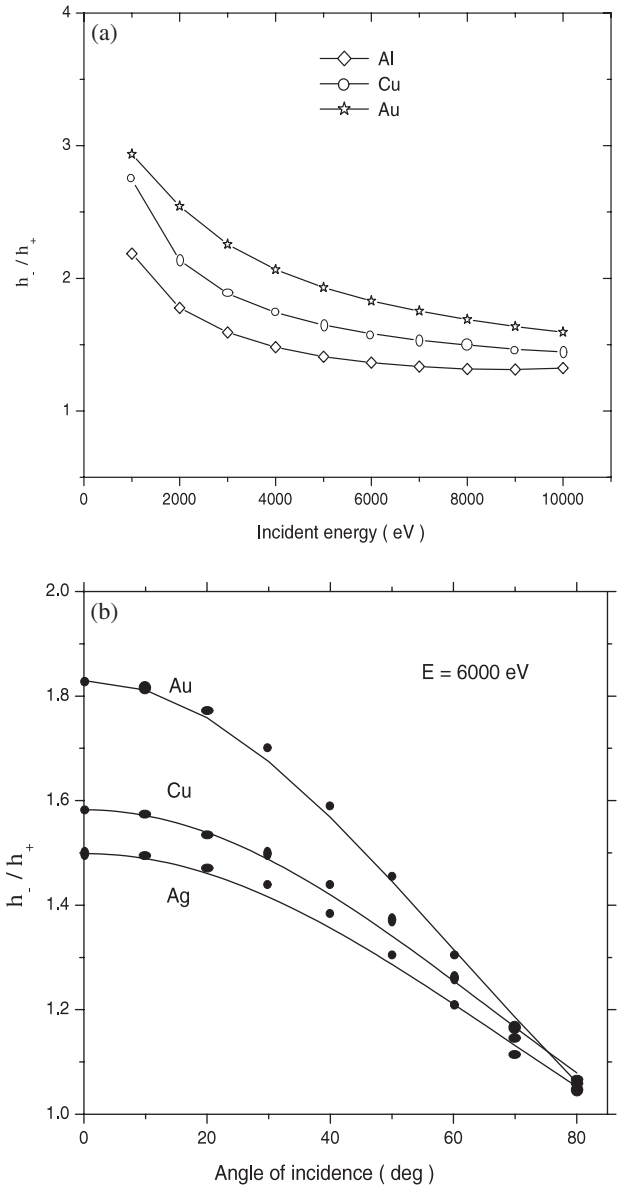

Figure 4. (a) Ratio of electron to positron backscattering coefficients versus projectile incident energy. (b) Ratio of electron to positron backscattering coefficients versus angle of incidence. The solid curves are fits of the calculated ratios to equation (6).

behaviour is common to all materials of interest. Note that, with the use of the results from equations (5) and (6), one might evaluate the electron and positron backscattering coefficients for a given material for oblique incident energies lower than 10 keV. However, it should be noted that, as shown in figure 4(a), the η_-/η_+ ratio is constant for projectile energies greater than 4 keV. We believe that for high projectile energies, the $\eta_-/\eta_+(Z)$ ratio is also constant and will not depend on Z. At high incident energies, our results predict a constant value of 1.3–1.5 for the η_-/η_+ ratio for all targets with $Z = 13$–79. Massoumi *et al* [34] and Coleman *et al* [21] confirm that a constant of 1.3 for $\eta_-/\eta_+(Z)$ is reasonable at high incident energies.

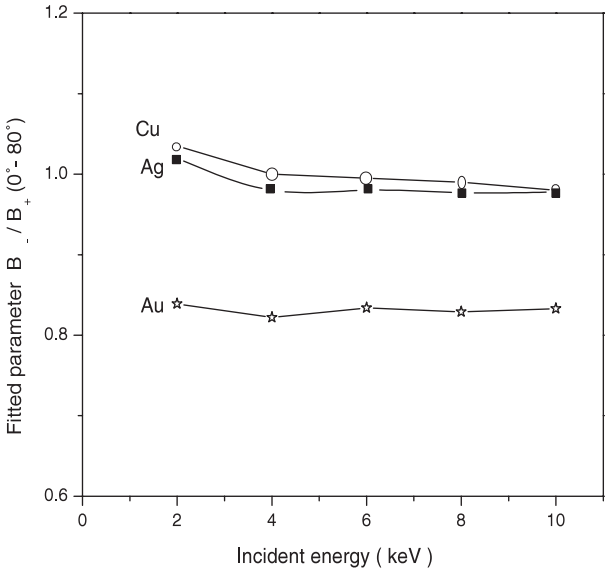

Figure 5. Fitted parameter $B_{\mp}$ deduced from equation (6) versus projectile incident energy. The solid curves are drawn to guide the eye.

4. Conclusion

On the basis of more realistic transport cross sections and the best fit functions for Ashley stopping powers, the analytical transport model of Vicanek and Urbassek is used to calculate backscattering coefficients of both electrons and positrons at energy 1–10 keV for a variety of species ($Z = 1$–79) for different incident angles.

A summary of the key findings follows:

(1) The calculated electron and positron backscattering coefficients showed very good agreement with experiment and were found to be better than earlier Monte Carlo simulations with respect to experiment as well as being less time-consuming to calculate.
(2) The backscattering coefficients are found to be sensitive to the choice of the incidence angle, showing the same qualitative behaviours of the electron and positron backscattering coefficients.
(3) The dependence of the ratio of electron to positron backscattering coefficients on the target atomic number was found to be significant at low energies while it is weak at high energies.

We therefore note that the analytical model used in the calculations works well and may give accurate results concerning backscattering coefficients of slow electrons and positrons impinging on solid targets. Thus the use of slow positrons as a probe for information on the surface or near-surface region is beneficial and very useful since the knowledge of the backscattering coefficient is necessary for the calculation of the backscattering of electrons (positrons) from thin films and multi-layers.

Acknowledgment

It is pleasure to thank Professor Hans Bichsel from the University of Washington, Seattle, Washington (USA), for providing us with preprints of recent papers.

References

[1] Niedrig H 1982 *J. Appl. Phys.* **53** R15
[2] Adesida I, Shimizu R and Everhart T E 1980 *J. Appl. Phys.* **51** 5962
[3] Schultz P J and Lynn K G 1988 *Rev. Mod. Phys.* **60** 701
[4] Tougaard S and Kraaer J 1991 *Phys. Rev.* B **43** 1651
[5] Powell C J, Jablonski A, Tanuma S and Penn D R 1994 *J. Electron Spectrosc. Relat. Phenom.* **68** 605
[6] Dapor M 1996 *J. Appl. Phys.* **79** 8406
[7] Rundgren J 1999 *Phys. Rev.* B **59** 5106
[8] Werner W S M 2001 *Surf. Interface Anal.* **31** 141
[9] Coleman P G 2002 *Appl. Surf. Sci.* **194** 264
[10] Gergely G 2002 *Prog. Surf. Sci.* **71** 31 and references cited therein
[11] Zecca A 2002 *Appl. Surf. Sci.* **194** 4
[12] Dapor M 1995 *Nucl. Instrum. Methods* B **95** 470
[13] Bouarissa N and Walker A B 2000 *Int. J. Mod. Phys.* B **14** 1603
[14] Chaoui Z and Bouarissa N 2002 *Phys. Lett.* A **297** 432
[15] Chaoui Z and Bouarissa N 2004 *Appl. Surf. Sci.* **221** 114
[16] Yasuda M, Kawata H and Murata K 1995 *J. Appl. Phys.* **77** 4706
[17] Mills A P Jr 1995 *Positron Spectroscopy of Solids* ed A Dupasquier and A P Mills Jr (Amsterdam: IOS) p 209
[18] Krause-Rehberg R and Leipner H S 1999 *Positron Annihilation in Semiconductors, Defect Studies* (Berlin: Springer)
[19] Weiss A H and Coleman P G 2000 *Positron Beams and their Applications* ed P G Coleman (Amsterdam: World Scientific) p 129
[20] Massoumi G R, Lennard W N, Schultz P J, Walker A B and Jensen K O 1993 *Phys. Rev.* B **47** 11007
[21] Coleman P G, Albrecht L, Jensen K O and Walker A B 1992 *J. Phys.: Condens. Matter* **4** 10311
[22] Bichsel H 1990 *Scanning Microsc.* **4** (Suppl.) 147
[23] Jensen K O, Walker A B and Bouarissa N 1990 *Positron Beams for Solids and Surfaces* (*AIP Conf. Proc.* vol 218) ed P J Schultz, G R Massoumi and P J Simpson (New York: American Institute of Physics) p 19
[24] Baker J A, Chilton N B, Jensen K O, Walker A B and Coleman P G 1991 *J. Phys.: Condens. Matter* **3** 4109
[25] Baker J A, Chilton N B, Jensen K O, Walker A B and Coleman P G 1991 *Appl. Phys. Lett.* **59** 2962
[26] Massoumi G R, Hozhabri N, Jensen K O, Lennard W N, Lorenzo M S, Schultz P J and Walker A B 1992 *Phys. Rev. Lett.* **68** 3873
[27] Dapor M 1992 *Phys. Rev.* B **46** 618
[28] Jensen K O and Walker A B 1993 *Surf. Sci.* **292** 83
[29] Ghosh V J and Aers G C 1995 *Phys. Rev.* B **51** 45
[30] Hunter K L, Snook I K and Wagenfeld H K 1996 *Phys. Rev.* B **54** 4507
[31] Bouarissa N, Walker A B and Aourag H 1998 *J. Appl. Phys.* **83** 3643
[32] Bouarissa N, Deghfel B and Bentabet A 2002 *Eur. Phys. J.: Appl. Phys.* **19** 89
[33] Bichsel H 2002 *Phys. Rev.* A **65** 052709
[34] Massoumi G R, Hozhabri N, Lennard W N and Schultz P J 1991 *Phys. Rev.* B **44** 3486
[35] Knights A P and Coleman P G 1995 *J. Phys.: Condens. Matter* **7** 3485
[36] Dapor M 2002 *Eur. Phys. J.: Appl. Phys.* **18** 155
[37] Dapor M 2003 *Nucl. Instrum. Methods* B **202** 155
[38] Deghfel B, Bentabet A and Bouarissa N 2003 *Phys. Status Solidi* b **238** 136
[39] Ashley J C 1990 *J. Electron. Spectrosc. Relat. Phenom.* **50** 323
[40] Vicanek M and Urbassek H M 1991 *Phys. Rev.* B **44** 7234
[41] Hohenberg P and Kohn W 1964 *Phys. Rev.* B **136** 864
Kohn W and Sham L J 1965 *Phys. Rev.* A **140** 1133
[42] Gunnarsson O and Lundqvist B I 1976 *Phys. Rev.* B **13** 4274
[43] Furness J B and MacCarthy I E 1973 *J. Phys. B: At. Mol. Phys.* **6** 2280
[44] Boronski E and Nieminen R M 1986 *Phys. Rev.* B **34** 3820
[45] Arponen J and Pajanne E 1979 *Ann. Phys.* **121** 343
[46] Valkealahti S and Nieminen R M 1984 *Appl. Phys.* A **35** 51
[47] Darlinski A 1981 *Phys. Status Solidi* a **63** 663
[48] Darlington E H and Cosslett V E 1972 *J. Phys. D: Appl. Phys.* **5** 1969